

# Cornwall-Jackiw-Tomboulis effective field theory to nonuniversal equation of state of an ultracold Bose gas

Yi Zhang<sup>1</sup> and Zhaoxin Liang<sup>1,\*</sup>

<sup>1</sup>*Department of Physics, Zhejiang Normal University, Jinhua 321004, People's Republic of China*  
(Dated: August 20, 2024)

The equation of state (EOS) serves as a cornerstone in elucidating the properties of quantum many-body systems. A recent highlight along this research line consists of the derivation of the nonuniversal Lee-Huang-Yang (LHY) EOS for an ultracold quantum bosonic gas with finite-range interatomic interactions using one-loop effective path-integral field theory [L. Salasnich, *Phys. Rev. Lett.* **118**, 130402 (2017)]. The purpose of this work is to extend Salasnich's pioneering work to uncover beyond-LHY corrections to the EOS by employing the Cornwall-Jackiw-Tomboulis (CJT) effective field theory, leveraging its two-loop approximation. In this end, we expand Salasnich's remarkable findings of EOS to the next leading order characterized by  $(\rho a_s^3)^2$ , with  $\rho$  and  $a_s$  being the density and the  $s$ -wave scattering length. Notably, we derive analytical expressions for quantum depletion and chemical potential, representing the next-to-LHY corrections to nonuniversal EOS induced by finite-range effects. Moreover, we propose an experimental protocol of observing the nonuniversal next-to-LHY corrections to the EOS by calculating fractional frequency shifts in the breathing modes. The nonuniversal beyond-LHY EOS in this work paves the way of using LHY effects in quantum simulation experiments and for investigations beyond the LHY regime.

## I. INTRODUCTION

The equation of state (EOS) of quantum physical systems, arising from quantum fluctuations, occupies a pivotal position at the very core of quantum many-body physics [1–3]. A prototypical illustration lies within the realm of quantum droplets [4–6] in the context of ultracold quantum gases. The basic principle underlying the stabilization of quantum droplets hinges on a delicate equilibrium between the attractive mean-field force and the repulsive force emanating from quantum fluctuations as described by the EOS [7–12]. Consequently, delving into the EOS can provide invaluable insights into the fundamental properties of quantum droplets, as evidenced across diverse systems, spanning from dipolar Bose gases [7–9] to Bose-Bose mixtures [10–12].

The interest in the EOS of ultracold quantum gases, particularly underscored by the aforementioned quantum droplets, can be traced back to the seminal works [13, 14] in the 1950s. Particularly, the Lee-Huang-Yang (LHY) correction to the EOS of weakly-interacting bosonic systems was first explored in Ref. [14]. In more details, the chemical potential has been derived to be proportional to  $[32/3\sqrt{\pi}] (\rho a_s^3)^{1/2}$  with  $a_s$  [15, 16] and  $\rho$  being the  $s$ -wave scattering length and the atomic density, respectively. Furthermore, the next-order correction to the energy density incorporates the universal quantum effect stemming from three-body correlations, yielding a term of  $\frac{8}{3} (4\pi - 3\sqrt{3}) \rho a_s^3 \ln[\rho a_s^3]$ , as outlined in Ref. [17]. Up to now, the highest-order term in the EOS has been derived in Ref. [18], which is given by  $[-512/3\pi] (\rho a_s^3) + [8192/9\pi^{3/2}] (\rho a_s^3)^{3/2}$ . At present,

there are the endless and ongoing research interests and efforts in obtaining beyond the mean-field terms of EOS of weakly-interacting bosonic systems motivated by the advent of well-controlled mixtures of quantum gases with tunable interaction strengths [19–23].

The EOS obtained in Refs. [13–18] are characterized by the universality, i.e. in more details, a single parameter  $a_s$ , eloquently encapsulates both the intricacies of the two-body interaction and, by extension, the overarching physics governing the many-body systems [24]. In sharp contrast, the nonuniversal EOS depends on other than the parameter  $a_s$ . The EOS of Bose gases becomes nonuniversal when the finite-range effects of the interatomic potential [25–29] is taken into account. In Refs. [26, 30], the analytical expressions of nonuniversal EOS are derived as  $[-64\sqrt{\pi}r_s/a_s] (\rho a_s^3)^{3/2}$ , featuring a nonuniversal LHY term in the quantum depletion. Given the tunability of the scattering length  $a_s$  [31, 32] through magnetic and optical Feshbach resonances [33–35] in ultracold atomic gases, the nonuniversal consequences stemming from the finite-range parameter  $r_s$  are of paramount importance. Consequently, an immediate challenge is referred as to calculating the next-to-LHY-order correction for the nonuniversal EOS.

The second impetus behind this paper stems from the measurement of collective excitation frequencies, which has emerged as an indispensable and highly accurate instrument for delving into the intricate EOS of atomic Bose-Einstein condensates (BECs) with unprecedented precision [15, 19–23, 36]. This approach not only solidifies the validity of mean-field predictions but also stands as an exceedingly potent technique to explore effects transcending the mean-field paradigm [37, 38]. From a theoretical standpoint, a gaseous BECs system can be aptly modeled by a single macroscopic wave function, thereby facilitating the derivation of clear-cut hy-

\* Corresponding author: zhxliang@zjnu.edu.cn

hydrodynamic formulations that yield analytical or semi-analytical insights into the dynamical characteristics of BECs systems. Thus, a timely and natural question arises as to observe the frequency shifts in the collective excitations induced by the nonuniversal beyond-LHY EOS, although tuning the finite-range interatomic interactions in this case remains experimentally challenging.

In this work, using Cornwall-Jackiw-Tomboulis (CJT) effective field theory [39–42], we are interested in the nonuniversal EOS [26, 28–30, 43] of a three-dimensional (3D) Bose gas with finite-range effective interactions at absolute zero temperature. Accordingly, we derive the analytical expressions of the quantum depletion and the chemical potential up to the order of  $(\rho a_s^3)^2$ . Our results not only include Salasnich’s remarkable EOS, but also give rise to nonuniversal beyond-LHY terms. Moreover, we explore the physical consequences of the nonuniversal beyond-LHY terms in EOS. As such, we extend the superfluid hydrodynamic equations by incorporating the aforementioned next-to-LHY corrections to the nonuniversal EOS. Leveraging these refined hydrodynamic equations, we delve into the fractional frequency shifts in the breathing modes, which are observable within the current experimental facilities. Observing this frequency shifts induced by the nonuniversal beyond-LHY EOS paves the way for a deeper understanding of quantum fluctuation of quantum many-body systems.

The paper is structured as follows. In Sec. II, we revisit the key principles of the CJT effective field theory

and subsequently derive the corresponding effective potential density for the model system. In Sec. III, we utilize the CJT effective potential within a two-loop approximation to deduce analytical expressions for the nonuniversal EOS. Sec. IV presents the fractional shift in the breathing mode frequency, aided by the next-to-LHY corrections to the nonuniversal chemical potential. Finally, in Sec. V, we provide a comprehensive summary of our paper and discuss the potential experimental conditions for realizing our proposed scenario.

## II. CORNWALL-JACKIW-TOMBOULIS EFFECTIVE FIELD THEORY

In this work, we are interested in a 3D weakly-interacting Bose gas, paying particular attention to the finite-range effects of the interatomic potential [27]. To investigate this system, we employ the path-integral formalism [1, 2], and the corresponding Euclidean partial function of the model system is presented below

$$\mathcal{Z} = \int \mathcal{D}[\phi, \phi^*] \exp \left\{ -\frac{S[\phi, \phi^*]}{\hbar} \right\}, \quad (1)$$

with the action functional  $S[\phi, \phi^*] = \int_0^{\beta\hbar} d\tau \int d^3\mathbf{r} \mathcal{L}$  in Eq. (1). Here, the concrete Lagrangian density  $\mathcal{L}$  denotes as follows [26, 30, 43, 44]

$$\mathcal{L}[\phi, \phi^*] = \phi^*(\mathbf{r}, \tau) \left[ \hbar \partial_\tau - \frac{\hbar^2 \nabla^2}{2m} - \mu \right] \phi(\mathbf{r}, \tau) + \frac{g_0}{2} |\phi(\mathbf{r}, \tau)|^4 - \frac{g_2}{2} |\phi(\mathbf{r}, \tau)|^2 \nabla^2 |\phi(\mathbf{r}, \tau)|^2. \quad (2)$$

In Equation (2), the complex field  $\phi(\mathbf{r}, \tau)$  represents the atomic bosons, varying in both space  $\mathbf{r}$  and imaginary time  $\tau$ . Here,  $\mu$  signifies the chemical potential, while  $\beta = 1/k_B T$  defines the inverse of the thermal energy scale, with  $k_B$  representing the Boltzmann constant and  $T$  denoting the temperature of the BECs. The parameters  $g_0 = 4\pi\hbar^2 a_s/m$  and  $g_2 = 2\pi\hbar^2 a_s^2 r_s/m$  [43], with  $a_s$  and  $r_s$  being the  $s$ -wave scattering length and the finite-range length respectively.

Note that the LHY correction to nonuniversal EOS of Lagrangian density functional (2) has already been derived [26, 30] within one-loop approximation, i.e. rewriting the partition function (1) in the form of  $\mathcal{Z} = e^{-\beta \mathcal{V} V_{\text{eff}}[\phi]}$ , with  $\mathcal{V}$  being the volume of the system. In this context, the effective potential  $V_{\text{eff}}[\phi]$  [45] within one-loop approximation solely relies on  $\phi(x)$ , which is the expected value of the quantum field  $\hat{\Psi}(x)$ .

In contrast, the emphasis and value of this paper lie in employing the CJT [40–42, 45, 46] effective action approach or the two particle-irreducible framework, surpassing the limitations of the one-loop approxima-

tion [45]. CJT theory enables us to compute the beyond-LHY corrections to the nonuniversal EOS for the Lagrangian density functional (2). A comprehensive introduction to the CJT effective field theory is provided in Appendix A.

The central step of CJT effective field theory [39–42] is to obtain the effective potential denoted as  $V_{\text{eff}}[\phi, G]$  (see Eq. (A9) in Appendix A) meticulously by taking into account both the background field  $\phi(x)$  and the dressed propagator  $G(x, y)$ . Here,  $G(x, y)$  is a potential expectation value of the time-ordered product  $T\hat{\Psi}^\dagger(x)\hat{\Psi}(y)$ . Then, physical solutions are ascertained by ensuring that the generalized effective potential satisfies the stationarity conditions:  $\delta V_{\text{eff}}/\delta\phi(x) = 0$ ,  $\delta V_{\text{eff}}/\delta G(x, y) = 0$ . Finally, at the core of the CJT effective field theory lies in the self-consistent loop expansion of the effective potential  $V_{\text{eff}}$ , intricately tied to the full propagator  $G$ . This expansion offers a powerful tool for systematically exploring higher-order corrections, thereby enhancing the accuracy and predictive capabilities of the system with finite-range effects taking into account. We remark that our

work, together with Refs. [26, 30], provides a complete description of the nonuniversal EOS of a 3D interacting Bose gas with finite-range effects of the interatomic potential.

The subsequent goal of Sec. II is to derive the effective potential  $V_{\text{eff}}$  for functional (2) within the framework of CJT effective field theory. Then, the obtained effective potential  $V_{\text{eff}}$  is used to calculate the nonuniversal beyond-LHY EOS.

The starting point of the CJT effective field theory commences with expressing the field  $\phi$  of functional (2) as a superposition of the condensate field  $\phi_0$  and real fluctuation fields of  $\phi_1$  and  $\phi_2$ , i.e.  $\phi = (\phi_0 + \phi_1 + i\phi_2)/\sqrt{2}$ . A rigorous methodology to attain  $V_{\text{eff}}$  involves executing a double Legendre transformation on the action functional  $S[\phi, \phi^*]$ , subjecting it to the conditions  $\delta V_{\text{eff}}/\delta\phi_0 = 0$  and  $\delta V_{\text{eff}}/\delta G = 0$ , where  $G$  represents a relevant variable (such as the two-point function or propagator) that may need to be optimized simultaneously with  $\phi_0$ . This ensures the effective potential accurately captures the dynamics of the system, incorporating both condensate and fluctuation effects.

Adhering closely to the established CJT effective field theory as outlined in Refs. [18, 46–49], we proceed by performing Fourier transformations on the fluctuation fields  $\phi_1$  and  $\phi_2$  to map them into the momentum-frequency domain. Subsequently, we select the Luttinger-Ward functional [45], denoted as  $\Phi[\phi_0, G]$ , as the foundational element. Consequently, the effective potential  $V_{\text{eff}}$  corresponding to partition function in Eq. (1) can be analytically formulated as (see the detailed derivation in Eq. (B8) in Appendix B)

$$\begin{aligned} V_{\text{eff}}[\phi_0, G] = & -\frac{\mu}{2}\phi_0^2 + \frac{g_0}{8}\phi_0^4 \\ & + \frac{1}{2}\int_{\beta}\text{Tr}[\ln G^{-1}(k) + G_0^{-1}(k)G(k) - \mathbf{1}] \\ & + \frac{3g_0}{8}(P_{11}^2 + P_{22}^2) + \frac{g_0}{4}P_{11}P_{22}. \end{aligned} \quad (3)$$

In Equation (3),  $k$  denotes the magnitude of the wave vector  $\mathbf{k}$ . The quantities  $G_0^{-1}(k)$  and  $G^{-1}(k)$  represent the inverse propagators within the one-loop and two-loop approximations, respectively. The notation  $\int_{\beta}$  encapsulates the integration over momentum space combined with a summation over bosonic Matsubara frequencies, specifically given by  $\int_{\beta} = \frac{1}{\beta}\sum_{n=-\infty}^{+\infty}\int\frac{d\mathbf{k}}{(2\pi)^3}$ ;  $\omega_n = 2\pi n\beta^{-1}$  are the Matsubara frequencies. The functions  $P_{aa} = \int_{\beta}G_{aa}(k)$  are termed momentum integrals, with  $a$  indexing the two fields (1, 2).

Minimizing the CJT effective potential  $V_{\text{eff}}$  in Eq. (3) with respect to the components of the propagator  $G(k)$ ,

we obtain

$$G^{-1}(k) = G_0^{-1}(k) + \Sigma. \quad (4)$$

In Equation (4), the context form of  $G_0^{-1}$  can be written as (see the detailed derivation in Eq. (B7) in Appendix B2)

$$G_0^{-1}(k) = \begin{bmatrix} \frac{\hbar^2 k^2}{2m} - \mu + \frac{3g_0}{2}\phi_0^2 + g_2\phi_0^2 k^2 & -\omega_n \\ \omega_n & \frac{\hbar^2 k^2}{2m} - \mu + \frac{g_0}{2}\phi_0^2 \end{bmatrix}. \quad (5)$$

Meanwhile,  $\Sigma$  in Eq. (4) represents the self-energy matrix in the form of

$$\Sigma = \begin{bmatrix} \Sigma_1 & 0 \\ 0 & \Sigma_2 \end{bmatrix}, \quad (6)$$

with the matrix entries  $\Sigma_1$  and  $\Sigma_2$  reading

$$\Sigma_1 = \frac{3g_0}{2}P_{11} + \frac{g_0}{2}P_{22}, \quad (7a)$$

$$\Sigma_2 = \frac{3g_0}{2}P_{22} + \frac{g_0}{2}P_{11}. \quad (7b)$$

Before proceeding with further calculations based on Eq. (3), we conduct a crucial verification to ensure that Eq. (3) can indeed reproduce the previous findings presented in Refs. [26, 30, 43]. Specifically, under the conditions where the propagator  $G(k)$  reduces to its bare form  $G_0(k)$  and both  $P_{11}$  and  $P_{22}$  vanish, the effective potential simplifies significantly to align with the one-loop approximation scenario. This simplification yields  $V_{\text{eff}}[\phi_0, G_0] = -\frac{\mu}{2}\phi_0^2 + \frac{g_0}{8}\phi_0^4 + \frac{1}{2}\int_{\beta}\text{Tr}\ln[G_0^{-1}(k)]$  within the context of the path-integral formalism. Then, after minimizing  $V_{\text{eff}}$  with respect to order parameter  $\phi_0$  and applying the thermodynamic relationship  $\rho = -\partial V_{\text{eff}}/\partial\phi_0$ , the nonuniversal EOS [26, 28–30, 43] can be obtained within one-loop approximation. Note that the CJT effective field theory not only introduces two-particle irreducible (2PI) terms in the last line of Eq. (3) but also modifies the propagator  $G$  in a more intricate manner, affecting the second term of  $V_{\text{eff}}$  in Eq. (3) in a complex and non-trivial way.

### III. NONUNIVERSAL EOS: CHEMICAL POTENTIAL AND QUANTUM DEPLETION

In the preceding Sec. II, we have delineated the framework of the CJT effective field theory. Moving forward, in Sec. III, our objective is to derive the explicit analytical expressions for the next-to-LHY-order correction to the nonuniversal EOS of a 3D Bose gas, utilizing the CJT effective potential of Eq. (3) within two-loop approximation. The starting point for this endeavor is to deduce the  $V_{\text{eff}}$  in Eq. (3) as (refer to Appendix B for a more comprehensive derivation),

$$V_{\text{eff}} = V_0 + \frac{1}{2} \int_{\beta} \text{Tr} [\ln G^{-1}(k)] + \frac{g_0}{8} (P_{11}^2 + P_{22}^2) + \frac{3g_0}{4} P_{11} P_{22} + \frac{1}{2} \left( -\mu + \frac{3g_0}{2} \phi_0^2 - M^2 \right) P_{11} + \frac{1}{2} \left( -\mu + \frac{g_0}{2} \phi_0^2 \right) P_{22}. \quad (8)$$

In Equation (8),  $V_0 = -\frac{\mu}{2} \phi_0^2 + \frac{g_0}{8} \phi_0^4$ ,  $P_{11} = \frac{\sqrt{2} m^{*3/2} M^3}{3\pi^2 \hbar^3} \sqrt{\frac{m^*}{m}}$  and  $P_{22} = \frac{-m^{*3/2} M^3}{3\sqrt{2}\pi^2 \hbar^3} \sqrt{\frac{m}{m^*}}$  (see Eqs. (B23a) and (B23b) in Appendix B for calculation details) with  $m^* = m / \left( 1 + \frac{2mg_2\phi_0^2}{\hbar^2} \right)$ .

The pivotal parameter  $M$  in Eq. (8) holds a crucial role in determining not only  $P_{11}$  and  $P_{22}$ , but also the other constituent terms in Eq. (8). Subsequently, we embark on deriving the precise expression for  $M$ , as outlined below:

(i). The parameter  $M$  in Eq. (8) fulfills the Schwinger-Dyson (SD) equation (as elaborated in detail in Eq. (B20) in Appendix B),

$$-\mu + \frac{3g_0}{2} \phi_0^2 + \frac{\sqrt{2}g_0 m^{*3/2} M^3}{12\pi^2 \hbar^3} \left( 2\sqrt{\frac{m^*}{m}} - 3\sqrt{\frac{m}{m^*}} \right) = M^2. \quad (9)$$

Equation (9) contains three variables, i.e.  $M$ ,  $\mu$ , and  $\phi_0$ . To ascertain their values, we require two additional equations in conjunction with Eq. (9).

(ii). Next, we proceed to seek for the second equation between  $M$ ,  $\mu$ , and  $\phi_0$ . Specifically, the chemical potential of  $\mu$  satisfies the gap equation by setting  $\delta V_{\text{eff}}/\delta \phi_0 = 0$  (for a detailed exposition, refer to Eq. (B13) in Appendix B),

$$-\mu + \frac{g_0}{2} \phi_0^2 + \frac{\sqrt{2}g_0 m^{*3/2} M^3}{12\pi^2 \hbar^3} \left( 6\sqrt{\frac{m^*}{m}} - \sqrt{\frac{m}{m^*}} \right) = 0. \quad (10)$$

$$M = \sqrt{2\rho g_0} \left\{ 1 - \frac{16}{3\sqrt{\pi} \left( 1 + 8\pi \frac{r_s}{a_s} \rho a_s^3 \right)^2} \sqrt{\rho a_s^3} \left[ 1 - \frac{40}{3\sqrt{\pi} \left( 1 + 8\pi \frac{r_s}{a_s} \rho a_s^3 \right)^2} \sqrt{\rho a_s^3} \right] + \mathcal{O} \left[ (\rho a_s^3)^{3/2} \right] \right\}. \quad (13)$$

In Equation (13), the effective mass  $M$ , emerges as a pivotal parameter characterizing weakly-interacting BECs. Our findings, encapsulated in Eq. (13) accurately reproduce previously established results in specific limiting cases. (i) In the absence of finite-range effects (i.e.  $r_s = 0$ ), we double check that our result aligns with Refs. [18, 49] in terms of the gas parameter  $\rho a_s^3$ . Firstly, in the limit where  $\rho a_s^3 \ll 1$ , Eq. (13) decouples from the gas parameter  $\rho a_s^3$ , contributing to the LHY term in the universal EOS. Secondly, under the additional constraint  $\rho a_s^3 \ll \sqrt{\rho a_s^3}$ , Eq. (13) truncates to the first order of  $\sqrt{\rho a_s^3}$ , contributing to the next-to-LHY term in the universal EOS. (ii) When the finite-range effects are con-

(iii). Finally, the third equation originated by determining the atomic density of  $\rho$ , can be obtained by taking the first-order derivative of the  $V_{\text{eff}}$  in Eq. (8) with respect to  $\mu$ ,

$$\rho = -\frac{\partial V_{\text{eff}}}{\partial \mu} = \frac{\phi_0^2}{2} + \frac{\sqrt{2} m^{*3/2} M^3}{12\pi^2 \hbar^3} \left( 2\sqrt{\frac{m^*}{m}} - \sqrt{\frac{m}{m^*}} \right). \quad (11)$$

Equations (9), (10) and (11) constitute a closed set of equations. By eliminating the variables  $\mu$  and  $\phi_0$  from Eq. (9) with the aid of Eqs. (10) and (11), we obtain a cubic equation solely in terms of  $M$ ,

$$M^3 + \frac{\left( 1 + 4 \frac{mg_2}{\hbar^2} \rho \right)^{3/2}}{8\sqrt{2} a_s m^{*1/2}} M^2 - \frac{3\pi^2 \hbar^3 \left( 1 + 4 \frac{mg_2}{\hbar^2} \rho \right)^{1/2}}{\sqrt{2} m^{*3/2}} \rho = 0, \quad (12)$$

with  $g_0 = 4\pi \hbar^2 a_s / m$  and  $m^* \simeq m / \left( 1 + 4m \frac{g_2}{\hbar^2} \rho \right)$ .

By solving Equation (12) using perturbation theory (details provided in Appendix C) and substituting  $g_2$  with  $2\pi \hbar^2 a_s^2 r_s / m$ , we derive the analytical expression of  $M$  expanded as the gas parameter  $\rho a_s^3$

sidered (i.e.  $r_s \neq 0$ ), our results accurately recover those in Ref. [30] when calculating the EOS of nonuniversal systems using the expression for  $M$ . This validation underscores the accuracy and applicability of our approach.

Having acquired the knowledge of  $M$  in Eq. (13), we are now poised to compute EOS of the model system, leveraging the CJT effective potential as presented in Eq. (8). Specifically, the EOS explored in this paper pertains to two key quantities: the quantum depletion, denoted as  $\rho_{\text{ex}}$ , and chemical potential, represented by  $\mu$ .

Using Equation (11), the expression for quantum depletion is given by  $\rho_{\text{ex}} = \frac{\sqrt{2} m^{*3/2} M^3}{12\pi^2 \hbar^3} \left( 2\sqrt{\frac{m^*}{m}} - \sqrt{\frac{m}{m^*}} \right)$ . By substituting the solution for  $M$  from Eq. (13) into

$\rho_{\text{ex}}$ , we derive the analytical expression for the quantum depletion expanded in terms of the gas parameter  $\rho a_s^3$

$$\rho_{\text{ex}} = \frac{8\rho}{3\sqrt{\pi}} (\rho a_s^3)^{1/2} - \frac{128\rho}{3\pi} (\rho a_s^3) + \frac{2048\rho}{9\pi^{3/2}} (\rho a_s^3)^{3/2} - 64\sqrt{\pi}\rho \frac{r_s}{a_s} (\rho a_s^3)^{3/2} + \frac{5120}{3} \rho \frac{r_s}{a_s} (\rho a_s^3)^2. \quad (14)$$

Next, integrating the gap equation from Eq. (10) with the thermodynamic relation for the density in Eq. (11), we systematically derive the analytical expression for the chemical potential. The expression for the chemical potential takes the form  $\mu = g_0\rho + g_0 \frac{\sqrt{2m^{*3/2}M^3}}{3\pi^2\hbar^3} \sqrt{\frac{m^*}{m}}$ . By plugging the expression for  $M$  from Eq. (13) into the formula of chemical potential, we are able to express  $\mu$  as an expansion in terms of the gas parameter  $\rho a_s^3$

$$\mu = g_0\rho \left[ 1 + \frac{32}{3\sqrt{\pi}} (\rho a_s^3)^{1/2} - \frac{512}{3\pi} (\rho a_s^3) + \frac{8192}{9\pi^{3/2}} (\rho a_s^3)^{3/2} - \frac{512}{3} \sqrt{\pi} \frac{r_s}{a_s} (\rho a_s^3)^{3/2} + \frac{16384}{3} \frac{r_s}{a_s} (\rho a_s^3)^2 \right] \quad (15)$$

Equations (14) and (15) embody the key analytical expressions for nonuniversal EOS of a weakly-interacting Bose gas, with finite-range effects taking into consideration. Our results of Eqs. (14) and (15), demonstrate their versatility by successfully recovering previously established results under specific limiting conditions. (i) In the absence of the finite-range effects (i.e.  $r_s = 0$ ), our results align perfectly with the Refs. [13, 14, 18, 49], as verified through the order of the gas parameter  $\rho a_s^3$ . First, at the leading order  $(\rho a_s^3)^0$ , all particles condense at the mean field  $\phi_0$ , resulting in zero excess density ( $\rho_{\text{ex}} = 0$ ) and chemical potential  $\mu = g_0\rho$ . Second, proceeding to the next order  $(\rho a_s^3)^{1/2}$ , Eq. (15) recovers the universal LHY term [13, 14]. Third, truncating at the order of  $(\rho a_s^3)^{3/2}$  for small gas parameter values, our results coincide with those reported in Ref. [18] as they should be, emphasizing the consistency and robustness of our approach. (ii) Then, when the finite-range effects are taken into account (i.e.  $r_s \neq 0$ ), our results maintain their consistency with the Refs. [26, 30, 43], expanded in terms of the gas parameter  $\rho a_s^3$ . Notably, truncating within the order of  $(\rho a_s^3)^{3/2}$ , the nonuniversal EOS in Eqs. (14) and (15) match precisely with those in Refs. [26, 30, 43], obtained via the functional path-integral method. Crucially, our approach offers a significant enhancement in precision. Not only do we approximate the universal EOS in Eqs. (14) and (15) up to the order of  $(\rho a_s^3)^{3/2}$ , but also uncover the nonuniversal next-to-LHY EOS, given by  $[16384r_s/3a_s] (\rho a_s^3)^2$ , utilizing the CJT effective field theory. This additional insight underscores the robustness and precision of our analytical framework.

Based on the chemical potential  $\mu$ , the inverse com-

pressibility  $\kappa^{-1} = \rho \frac{\partial \mu}{\partial \rho}$  can be readily derived

$$\kappa^{-1} = g_0\rho \left[ 1 + \frac{3}{2} \alpha \rho^{1/2} - 3\alpha^2 \rho + \frac{15}{8} \alpha^3 \rho^{3/2} - \frac{45\pi^2}{128} \frac{r_s}{a_s} \alpha^3 \rho^{3/2} + \frac{81\pi^2}{64} \frac{r_s}{a_s} \alpha^4 \rho^2 \right], \quad (16)$$

with  $\alpha = (32/3\sqrt{\pi}) a_s^{3/2}$ .

To delve deeper into our analysis, utilizing the Eq. (16), we explore the nonuniversal quantum effect present in the speed of sound, denoted as  $c_s = \sqrt{(\kappa m)^{-1}}$ ,

$$c_s = \sqrt{\frac{g_0\rho}{m}} \left\{ 1 + \frac{8\sqrt{\rho a_s^3}}{\sqrt{\pi}} \left[ 1 - \frac{64\sqrt{\rho a_s^3}}{3\sqrt{\pi}} + \frac{1280}{9\pi} \rho a_s^3 - \frac{80\pi}{3} \frac{r_s}{a_s} \rho a_s^3 + 1024\sqrt{\pi} \frac{r_s}{a_s} \sqrt{\rho a_s^3} \right] \right\} \quad (17)$$

In Equation (17), the coefficient associated with the term  $\sqrt{\rho a_s^3}$  is  $8/\sqrt{\pi}$ , differing from LHY's prediction of  $16/\sqrt{\pi}$ . The deviation is readily traceable to the corresponding corrective terms present in the definition of the inverse compressibility  $\kappa^{-1}$ , given by Eq. (16). As a consequence of the nonuniversal effect, our derived expression for the sound speed  $c_s$  incorporates higher-order terms in the gas parameter  $\rho a_s^3$ , distinguishing it from the findings presented in Ref. [49]. This feature underscores the paramount importance and significance of our approach.

#### IV. FREQUENCY SHIFTS INDUCED BY NONUNIVERSAL BEYOND-LHY EOS

In Sec. III, we have rigorously derived the nonuniversal next-to-LHY terms in EOS (see Eqs. (14) and (15)) to the order of  $(\rho a_s^3)^2$ . The purpose of Sec. IV is to propose an experimental protocol to observe the nonuniversal beyond-LHY corrections to the EOS by calculating the frequency shifts in the breathing modes. In contemporary experiments, the gas parameter  $\rho a_s^3$  typically remains below  $10^{-4}$ , rendering even the initial LHY correction to the mean-field energy, scaling as  $\sqrt{\rho a_s^3}$ , negligible at best, contributing less than 1% of the total energy. Consequently, the higher-order corrections beyond LHY in Eq. (15) are anticipated to be too subtle to discern in density profiles or release energies. While enhancing quantum fluctuations by tuning  $a_s$  via Feshbach resonance [31–35, 50] can amplify their impact, we propose an alternative route: studying the frequency shifts in collective excitations [51–54] induced by quantum fluctuations [55]. To this end, we augment our model system with a 3D harmonic trap, defined by  $V_{\text{ext}} = \frac{1}{2}m\omega_0^2 r^2$ , and embark on calculating the resulting shifts in the breathing mode frequency, attributed to beyond-LHY terms in Eq. (15). This endeavor is motivated by the potential

to experimentally verify and quantify the nonuniversal contributions to the EOS.

Adhering closely to the standard methodology outlined in Ref. [38] for calculating frequency shifts, we formulate the hydrodynamic equation as follows:

$$m \frac{\partial^2 \delta \rho(\mathbf{r}, t)}{\partial t^2} - \nabla \cdot \left[ \rho(\mathbf{r}) \nabla \left( \frac{\partial \mu_l}{\partial \rho} \delta \rho(\mathbf{r}, t) \right) \right] = 0. \quad (18)$$

Equation (18) incorporates the density fluctuation, denoted as  $\delta \rho(\mathbf{r}, t)$ , which arises around the targeted ground state density  $\rho(\mathbf{r})$  and the local chemical potential  $\mu_l$  as specified in Eq. (15).

As an initial step, utilizing Eq. (15), we can iteratively derive the expansion of the ground state, expressed in

terms of  $\alpha = (32/3\sqrt{\pi}) a_s^{3/2}$ ,

$$\begin{aligned} \rho(\mathbf{r}) = & \rho_{\text{TF}} - \alpha \rho_{\text{TF}}^{3/2} + \frac{3}{2} \alpha^2 \rho_{\text{TF}}^2 - \frac{3}{4} \alpha^3 \rho_{\text{TF}}^{5/2} \\ & + \frac{9}{64} \pi^2 \frac{r_s}{a_s} \alpha^3 \rho_{\text{TF}}^{5/2} - \frac{27}{64} \pi^2 \frac{r_s}{a_s} \alpha^4 \rho_{\text{TF}}^3. \end{aligned} \quad (19)$$

In Equation (19),  $\rho_{\text{TF}} = (g_0 \rho - V_{\text{ext}})/g_0$  [37, 38], is the so-called Thomas-Fermi result for the ground state density. Examining Eq. (19), we observe that its first line comprises three distinct terms: the mean-field term being  $\rho_{\text{TF}}$ , the universal LHY term represented by  $-\alpha \rho_{\text{TF}}^{3/2}$ , and the universal beyond-LHY term  $3/2 \alpha^2 \rho_{\text{TF}}^2 - 3/4 \alpha^3 \rho_{\text{TF}}^{5/2}$ . Notably, the second line of Eq. (19) vanishes solely when nonuniversal effects are disregarded, emphasizing their significance. Consequently,  $\frac{9}{64} \pi^2 \frac{r_s}{a_s} \alpha^3 \rho_{\text{TF}}^{5/2}$  is designated as the nonuniversal LHY term, while  $-\frac{27}{64} \pi^2 \frac{r_s}{a_s} \alpha^4 \rho_{\text{TF}}^3$  corresponds to the nonuniversal next-to-LHY term.

Subsequently, we derive the expansion of  $[\rho \partial \mu_l / \partial \rho]$  as a series in terms of  $\rho_{\text{eff}}$  by substituting Eq. (19) into Eq. (16). Following this substitution, we insert both Eqs. (16) and (19) into the Eq. (18). Through meticulous algebraic manipulations, we ultimately arrive at

$$\begin{aligned} m \omega^2 \delta \rho + \nabla \cdot [g_0 \rho_{\text{TF}} \nabla \delta \rho] = & -\frac{1}{2} \alpha \nabla^2 (g_0 \rho_{\text{TF}}^{3/2} \delta \rho) + \frac{15}{4} \alpha^2 \nabla^2 (g_0 \rho_{\text{TF}}^2 \delta \rho) - 3 \alpha^2 \nabla \cdot (g_0 \rho_{\text{TF}} \delta \rho \nabla \rho_{\text{TF}}) \\ & + \left( -\frac{45}{4} + \frac{63 \pi^2 r_s}{128 a_s} \right) \alpha^3 \nabla^2 (g_0 \rho_{\text{TF}}^{5/2} \delta \rho) + \frac{57}{4} \alpha^3 \nabla \cdot (g_0 \rho_{\text{TF}}^{3/2} \delta \rho \nabla \rho_{\text{TF}}) \\ & + \left( \frac{165}{8} - \frac{261 \pi^2 r_s}{128 a_s} \right) \alpha^4 \nabla^2 (g_0 \rho_{\text{TF}}^3 \delta \rho) + \left( -\frac{495}{16} + \frac{27 \pi^2 r_s}{16 a_s} \right) \alpha^4 \nabla \cdot (g_0 \rho_{\text{TF}}^2 \delta \rho \nabla \rho_{\text{TF}}) \end{aligned} \quad (20)$$

Equation (20) simplifies into the basic hydrodynamic equation  $m \omega^2 \delta \rho + \nabla \cdot [\rho_{\text{TF}} \nabla g_0 \delta \rho] = 0$  in case of  $\alpha = 0$ . For this simplified scenario, the calculated frequency  $\omega$  exhibits analytical solutions of the form  $\omega(n_r, l) = \omega_0 (2n_r^2 + 2n_r l + 3n_r + l)^{1/2}$ , with  $n_r$  representing the number of radial nodes and  $l$  denoting the angular mo-

mentum associated with the excitation. This analytical expression provides a direct link between the frequency of the excitation and its quantum numbers.

Finally, Equation (20) can be routinely tackled by considering its right-hand side as a minor perturbation. By adopting this approach, we can derive the analytical expression for the frequency shifts,

$$\begin{aligned} \frac{\delta \omega}{\omega} = & -\frac{\alpha g_0}{4m\omega^2} \frac{\int d^3 \mathbf{r} \nabla^2 (\delta \rho^*) \rho_{\text{TF}}^{3/2} \delta \rho}{\int d^3 \mathbf{r} \delta \rho^* \delta \rho} + \frac{15 \alpha^2 g_0}{8m\omega^2} \frac{\int d^3 \mathbf{r} \nabla^2 (\delta \rho^*) \rho_{\text{TF}}^2 \delta \rho}{\int d^3 \mathbf{r} \delta \rho^* \delta \rho} + \frac{3 \alpha^2 g_0}{2m\omega^2} \frac{\int d^3 \mathbf{r} \nabla (\delta \rho^*) \cdot \nabla (\rho_{\text{TF}}) \rho_{\text{TF}} \delta \rho}{\int d^3 \mathbf{r} \delta \rho^* \delta \rho} \\ & + \frac{\left( -\frac{45}{4} + \frac{63 \pi^2 r_s}{128 a_s} \right) \alpha^3 g_0}{2m\omega^2} \frac{\int d^3 \mathbf{r} \nabla^2 (\delta \rho^*) \rho_{\text{TF}}^{5/2} \delta \rho}{\int d^3 \mathbf{r} \delta \rho^* \delta \rho} - \frac{\frac{57}{4} \alpha^3 g_0}{2m\omega^2} \frac{\int d^3 \mathbf{r} \nabla (\delta \rho^*) \cdot \nabla (\rho_{\text{TF}}) \rho_{\text{TF}}^{3/2} \delta \rho}{\int d^3 \mathbf{r} \delta \rho^* \delta \rho} \\ & + \frac{\left( \frac{165}{8} - \frac{261 \pi^2 r_s}{128 a_s} \right) \alpha^4 g_0}{2m\omega^2} \frac{\int d^3 \mathbf{r} \nabla^2 (\delta \rho^*) \rho_{\text{TF}}^3 \delta \rho}{\int d^3 \mathbf{r} \delta \rho^* \delta \rho} - \frac{\left( -\frac{495}{16} + \frac{27 \pi^2 r_s}{16 a_s} \right) \alpha^4 g_0}{2m\omega^2} \frac{\int d^3 \mathbf{r} \nabla (\delta \rho^*) \cdot \nabla (\rho_{\text{TF}}) \rho_{\text{TF}}^2 \delta \rho}{\int d^3 \mathbf{r} \delta \rho^* \delta \rho}. \end{aligned} \quad (21)$$

The integrals in Eq. (21) are confined to the domain

where the Thomas-Fermi density remains positive. To

delve into effects that transcend the LHY theory, it becomes imperative to concentrate on compressional modes, which are highly responsive to alterations in the EOS. Among these, the breathing mode in a spherical trap, characterized by  $(n_r = 1, l = 0)$ , stands as the fundamental excitation. This mode is distinguished by its zeroth-order dispersion, yielding a frequency of  $\omega = \sqrt{5}\omega_0$  and exhibits density oscillations that adhere to the pattern  $\delta\rho \sim (r^2 - 3/5R^2)$ . In this specific scenario, Eq. (21) furnishes:

$$\begin{aligned} \frac{\delta\omega}{\omega} = & \frac{63\sqrt{\pi}}{128} [\rho(0) a_s^3]^{1/2} - \frac{16384}{135\pi} [\rho(0) a_s^3] \\ & + \frac{3682 - \frac{2205}{16}\pi^2 \frac{r_s}{a_s}}{3\sqrt{\pi}} [\rho(0) a_s^3]^{3/2} \\ & + \left( \frac{-71200}{\pi^2} + 6465 \frac{r_s}{a_s} \right) [\rho(0) a_s^3]^2, \quad (22) \end{aligned}$$

revealing the fractional shift in the breathing mode frequency, where  $\rho(0)$  represents the density evaluated at the center of the trap.

Equation (22) constitutes another pivotal finding, encapsulating corrections to the breathing mode frequency that scale with the gas parameter  $\rho(0) a_s^3$ . The corrections in Eq. (22) stem from diverse origins, encompassing both LHY and beyond-LHY contributions to the EOS. The first term on the right-hand side of Eq. (22) represents the ubiquitous LHY-mediated fractional shift of the breathing mode frequency, which scales as  $[\rho(0) a_s^3]^{1/2}$ . All the subsequent terms in Eq. (22) are of higher order than  $[\rho(0) a_s^3]^{1/2}$ , offering insights into more intricate effects. Notably, among these beyond-LHY terms, the one scaling with  $[\rho(0) a_s^3]$  is a so-called next-to-LHY universal fractional shift. This term, specifically  $\frac{-16384}{135\pi} [\rho(0) a_s^3]$ , underscores the persistence of universal behavior beyond the leading LHY correction. Particularly, terms in Eq. (22) involving  $r_s$  represent nonuniversal contributions, arising from the finite-range effective potential, further illuminating the intricacies of the system's response. Thus, the complexity deepens with the term  $\frac{3682 - \frac{2205}{16}\pi^2 \frac{r_s}{a_s}}{3\sqrt{\pi}} [\rho(0) a_s^3]^{3/2}$  in Eq. (22), which encapsulates both the next-next-to-LHY universal fractional shift  $\frac{3682}{3\sqrt{\pi}} [\rho(0) a_s^3]^{3/2}$  and a next-to-LHY nonuniversal contribution  $\frac{-2205}{3\sqrt{\pi}} \pi^2 \frac{r_s}{a_s} [\rho(0) a_s^3]^{3/2}$ . Similarly, the last term  $\left( \frac{-71200}{\pi^2} + 6465 \frac{r_s}{a_s} \right) [\rho(0) a_s^3]^2$  in Eq. (22) comprises two distinct components: the next-next-next-to-LHY universal fractional shift  $\frac{-71200}{\pi^2} [\rho(0) a_s^3]^2$  and the next-next-next-to-LHY nonuniversal fractional shift  $6465 \frac{r_s}{a_s} [\rho(0) a_s^3]^2$ . We remark that to our best knowledge, the analytical expressions of beyond-LHY-induced fractional shift of the breathing mode frequency in Eq. (22) are obtained for the first time.

Before delving into the intricacies concerning the fractional shift in the breathing mode frequency as described in Eq. (22), it is crucial to assess the rationality of the di-

mensionless finite-range coupling constant  $r_s/a_s$  and the gas parameter  $\rho(0) a_s^3$ . This preliminary examination is fundamental as it sheds light on the experimental feasibility of our proposed model. To exemplify, let us take the case of  ${}^6\text{Li}$ , as mentioned in Ref. [56]. In this context, the typical density  $\rho(0)$  is approximately  $4 \times 10^{12} \text{cm}^{-3}$ , while the scattering length  $a_s$  is estimated to be approximately  $1.13 \times 10^{-7} \text{m}$ . Consequently, the magnitude of  $\rho(0) a_s^3$  falls within the order of  $10^{-3}$ . Furthermore, according to Ref. [57], the effective distance  $r_s$  is estimated to lie within the interval of  $0 \sim \pm 3.71 \times 10^{-6} \text{m}$ . By substituting these parameters into the expressions for  $r_s/a_s$  and  $\rho(0) a_s^3$ , we can reasonably infer that  $r_s/a_s$  falls within the range of  $0 \sim \pm 1$ . This assessment underscores the physical relevance and potential experimental applicability of our model's key parameters.

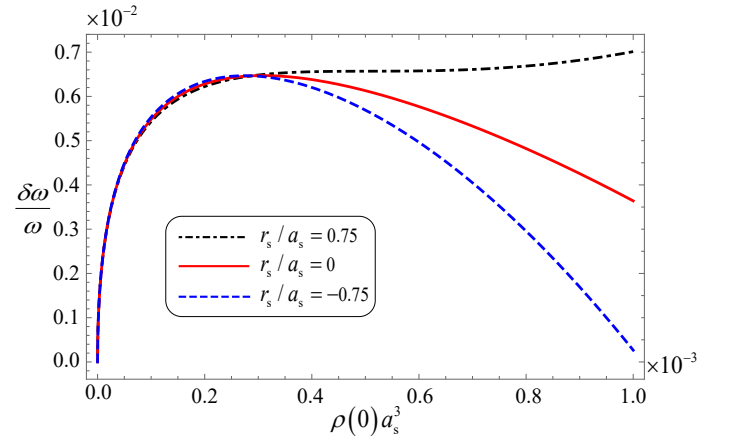


Figure 1. Frequency shifts  $\delta\omega/\omega$  as a function of the gas parameter  $\rho a_s^3$  with different values of  $r_s/a_s$ . All the curves are plotted by Eq. (22), showing the frequency shifts in breathing modes arising from the nonuniversal beyond-LHY EOS of a 3D Bose gas.

We are now poised to discuss the influence of the nonuniversal EOS in Eq. (15), stemming from the finite-range interaction parameter  $r_s$ , on the fractional shift of the breathing mode frequency in Eq. (22). To visualize this effect, we have plotted frequency shifts of the breathing mode  $\delta\omega/\omega$  in Eq. (22) into Fig. 1, showing how the dimensionless finite-range interaction parameter of  $r_s/a_s$  can affect the frequency shifts of  $\delta\omega/\omega$ . Note that the red solid curve in Fig. 1 corresponds to case of vanishing the finite-range interaction by taking the dimensionless parameter of  $r_s/a_s = 0$ ; meanwhile the black dot-dashed and blue dashed curves in Fig. 1 demonstrate how the repulsive ( $r_s/a_s = 0.75$ ) and attractive ( $r_s/a_s = -0.75$ ) finite-range interaction can affect frequency shifts of  $\delta\omega/\omega$ . As shown in Fig. 1, the finite-range interaction has relative small effects on frequency shifts of  $\delta\omega/\omega$  compared with the case of vanishing the finite-range interaction when the gas parameter of  $\rho a_s^3$  is small. In contrast, with the increase of the  $\rho a_s^3$ , the effect of finite-range interaction on frequency shifts of  $\delta\omega/\omega$

becomes to be significant. For example, at the typical experimental parameter onset of  $\rho a_s^3 \sim 10^{-3}$ , the derivation of the fractional shift of  $\delta\omega/\omega$  in case of  $r_s/a_s = 0.75$  from the case of  $r_s/a_s = 0$  is calculated as more than 0.5%, showing the finite-range effect well in reach in experiments. We point out that a precision of  $< 0.3\%$  in measuring collective frequencies has already been established [19–23], offering opportunities to probe the nonuniversal beyond-LHY corrections to EOS experimentally.

## V. CONCLUSION AND OUTLOOK

In summary, we have theoretically investigated the nonuniversal EOS for a weakly-interacting Bose gas with the finite-range interatomic interaction. With the framework of CJT effective field theory under the two-loop approximation, we obtain analytical expressions for quantum depletion and chemical potential of model system, representing the next-to-LHY correction to nonuniversal EOS induced by finite-range effects. These analytical results represent significant generalizations of the nonuniversal LHY EOS studied in Refs. [26, 30, 43] to the beyond LHY regimes, offering fresh insights into understanding the quantum behavior induced by the quantum fluctuations in many-body bosonic systems. We further calculate the frequency shifts in the breathing mode induced by the nonuniversal beyond-LHY EOS. Therefore, the beyond-LHY effects studied in this work should be

observable within the current experiment capability.

We finally remark that the CJT theory developed in this work can be readily applied to other ultracold quantum systems, including the novel quantum droplet phases of interacting Bose mixtures or ultracold quantum Fermi systems. Our results lay the groundwork for further investigation of the nonuniversal beyond-LHY EOS.

We thank Xiaoran Ye, Tao Yu and Ying Hu for stimulating discussions. This work was supported by the National Natural Science Foundation of China (Nos. 12074344), the Zhejiang Provincial Natural Science Foundation (Grant Nos. LZ21A040001) and the key projects of the Natural Science Foundation of China (Grant No. 11835011).

## Appendix A: CJT EFFECTIVE FIELD THEORY

For the purpose of maintaining self-consistency within this work, we provide a concise overview of the key steps of the Cornwall-Jackiw-Tomboulis (CJT) effective field theory, drawing from seminal works (see e.g. Refs. [39, 40] and the references therein). Specifically, we delve into the detailed derivation of the effective potential  $V_{\text{eff}}$  as presented in Eq. (3), elucidating each step to ensure a comprehensive understanding.

To begin with, let us contemplate the partition function, which incorporates both linear and bilinear external sources,

$$\mathcal{Z}[J, K] = e^{-W[J, K]/\hbar} = \int \mathcal{D}[\Psi] \exp \left\{ -\frac{1}{\hbar} \left[ \int d^4x \mathcal{L}[\Psi] + J(x) \Psi(x) + \frac{1}{2} \int d^4x d^4y \Psi(x) K(x, y) \Psi(y) \right] \right\}. \quad (\text{A1})$$

In Equation (A1),  $\int d^4x = \int_0^{\beta\hbar} d\tau \int d^3\mathbf{r}$ . So that we have

$$\frac{\delta W[J, K]}{\delta J(x)} = -\frac{\delta \ln \mathcal{Z}}{\delta J(x)} = \langle \Psi(x) \rangle_{J, K} = \phi(x), \quad (\text{A2a})$$

$$\begin{aligned} \frac{\delta W[J, K]}{\delta K(x, y)} &= -\frac{\delta \ln \mathcal{Z}}{\delta K(x, y)} = \frac{1}{2} \langle \Psi(x) \Psi(y) \rangle_{J, K} \\ &= \frac{1}{2} [\phi(x) \phi(y) + \hbar G(x, y)]. \end{aligned} \quad (\text{A2b})$$

The effective action, denoted as  $\Gamma[\phi, G]$ , is precisely defined through the application of the double Legendre transformation to the generating functional  $W[J, K]$ . This transformation yields the expression:

$$\begin{aligned} \Gamma[\phi, G] &= W[J, K] - \int d^4u \phi(u) J(u) \\ &\quad - \frac{1}{2} \int d^4v d^4w K(v, w) [\phi(v) \phi(w) + \hbar G(v, w)], \end{aligned} \quad (\text{A3})$$

which is subject to the conditions encapsulated in the

following set of equations:

$$\frac{\delta \Gamma[\phi, G]}{\delta \phi(x)} = -J(x) - \int d^4w K(x, w) \phi(w), \quad (\text{A4a})$$

$$\frac{\delta \Gamma[\phi, G]}{\delta G(x, y)} = -\frac{1}{2} \hbar K(x, y). \quad (\text{A4b})$$

Equations (A4a) and (A4b) underscore the intricate relationship between the effective action and its functional derivatives with respect to the classical field  $\phi$  and the two-point function  $G$ , respectively. After the saddle-point approximation, we calculate  $\mathcal{Z}$  as

$$\begin{aligned} \mathcal{Z} &\simeq e^{-S[\phi, J, K]/\hbar} \int \mathcal{D}[\tilde{\Psi}] e^{-\frac{1}{2\hbar} \int d^4x d^4y \tilde{\Psi}(x) [D_0^{-1} + K] \tilde{\Psi}(y)} \\ &= e^{-S[\phi, J, K]/\hbar} [\det [(D_0^{-1} + K) / \hbar]]^{-1/2}, \end{aligned} \quad (\text{A5})$$

with

$$S[\phi, J, K] = \int d^4x \phi D_0^{-1} \phi + \int d^4x d^4y \phi \frac{K}{2} \phi + \int d^4x J \phi. \quad (\text{A6})$$

Plugging Eqs. (A6) and (A5) into Eq. (A3), we can obtain

$$\Gamma[\phi, G] = \frac{1}{2} \int d^4x \phi D_0^{-1} \phi + \frac{\hbar}{2} \text{Tr} \ln [(D_0^{-1} + K)] - \frac{\hbar}{2} \int d^4v d^4w K(v, w) G(v, w). \quad (\text{A7})$$

By taking the logarithm of Eq. (A5) and subsequently computing its first-order derivative with respect to  $K(x, y)$ , utilizing Eq. (A6) as an aid, we can establish a direct comparison with Eq. (A2b). This comparison leads to the conclusion that  $G^{-1} = D_0^{-1} + K$ . Consequently,  $\Gamma[\phi, G]$  can be expressed as

$$\begin{aligned} \Gamma[\phi, G] &= \frac{1}{2} \int d^4x \phi D_0^{-1} \phi \\ &+ \frac{\hbar}{2} \text{Tr} [\ln G^{-1} + D_0^{-1} G - \mathbf{1}] \\ &+ \mathcal{I}[\phi, G], \end{aligned} \quad (\text{A8})$$

where  $\mathcal{I}[\phi, G]$  is the Luttinger-Ward functional. However, our primary focus lies solely on translation-invariant solutions. To this end, we simplify our analysis by setting  $\phi(x)$  to a constant value, denoted as  $\phi_0$ , and considering  $G(x, y)$  as a function exclusively dependent on the difference  $x - y$ . This specific choice allows us to define a generalized form of the effective potential as

$$\begin{aligned} V_{\text{eff}} &= \frac{1}{\beta \hbar \mathcal{V}} \Gamma[\phi_0, G] \\ &= \frac{1}{2} \phi_0 D_0^{-1} \phi_0 + \frac{1}{\beta \mathcal{V}} \left[ \frac{1}{2} \text{Tr} (\ln G^{-1} + D_0^{-1} G - \mathbf{1}) \right] \\ &+ \Phi[\phi_0, G]. \end{aligned} \quad (\text{A9})$$

with  $\Phi[\phi_0, G]$  being the average of time and space of the  $\mathcal{I}[\phi_0, G]$ .

## Appendix B: DETAILED DERIVATION OF THE EFFECTIVE POTENTIAL $V_{\text{eff}}$ OF EQ. (8)

To ensure the self-consistency and comprehensiveness of this work, we provide a concise overview of the crucial steps involved in deriving the self-consistent  $V_{\text{eff}}$  that fulfills the condition of gapless excitations (see e.g. Refs. [18, 58] and the references therein). In particular, we delve into the derivation of the effective potential  $V_{\text{eff}}$  as presented in Eq. (8). To effectively implement the CJT effective field theory [39], it is advantageous to initially transform the CJT effective potential density into the momentum-frequency space

$$\phi_1(\mathbf{r}, \tau) = \sqrt{\frac{1}{\beta \hbar \mathcal{V}}} \sum_{\mathbf{k}, \omega_n} e^{i\mathbf{k}\cdot\mathbf{r} + i\omega_n \tau / \hbar} \phi_1(\mathbf{k}, \omega_n) \quad (\text{B1a})$$

$$\phi_2(\mathbf{r}, \tau) = \sqrt{\frac{1}{\beta \hbar \mathcal{V}}} \sum_{\mathbf{k}, \omega_n} e^{i\mathbf{k}\cdot\mathbf{r} + i\omega_n \tau / \hbar} \phi_2(\mathbf{k}, \omega_n) \quad (\text{B1b})$$

with  $\beta$  defined as  $1/k_B T$ , where  $k_B$  is the Boltzmann constant and  $T$  represents the temperature,  $\mathcal{V}$  denotes the volume of the system under consideration. Furthermore,  $k$  signifies the magnitude of the wave vector  $\mathbf{k}$ , while  $\omega_n = 2\pi n/\beta$  represents the bosonic Matsubara frequency, with  $n$  being integers. This transformation facilitates a more streamlined analysis and allows us to leverage the properties of Fourier transforms in our calculations.

Based on the CJT effective field theory, we find the CJT effective potential density from the Lagrangian density (2) as

$$\begin{aligned} V_{\text{eff}}[\phi_0, G] &= -\frac{\mu}{2} \phi_0^2 \\ &+ \frac{1}{2} \int_{\beta} \text{Tr} [\ln G^{-1}(k) + D_0^{-1}(k) G(k) - \mathbf{1}] \\ &+ \Phi[\phi_0, G], \end{aligned} \quad (\text{B2})$$

with  $\Phi[\phi_0, G]$  being the Luttinger-Ward functional as shown in Fig. 2.

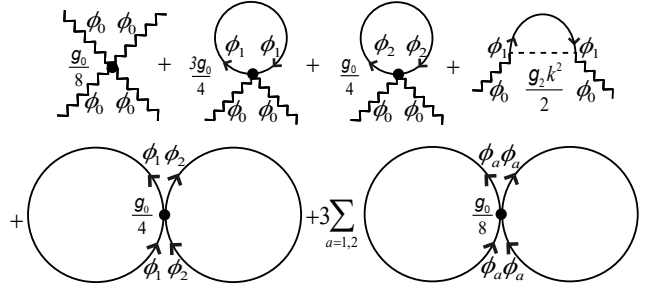


Figure 2. Feynman 2PI diagrams corresponding to Luttinger-Ward functional of  $\Phi[\phi_0, G]$  in Eq. (B2).

More specifically,  $\Phi[\phi_0, G] = \frac{g_0}{8} \phi_0^4 + \frac{3g_0}{4} \phi_0^2 P_{11} + \frac{g_0}{4} \phi_0^2 P_{22} + \frac{g_2}{2} \phi_0^2 k^2 P_{11} + \frac{g_0}{4} P_{11} P_{22} + \frac{3g_0}{8} (P_{11}^2 + P_{22}^2)$ , where the functions  $P_{11}$  and  $P_{22}$  denote as

$$P_{11} = \int_{\beta} G_{11}(k) = \frac{1}{\beta} \sum_{n=-\infty}^{+\infty} \int \frac{d\mathbf{k}}{(2\pi)^3} G_{11}(k) \quad (\text{B3a})$$

$$P_{22} = \int_{\beta} G_{22}(k) = \frac{1}{\beta} \sum_{n=-\infty}^{+\infty} \int \frac{d\mathbf{k}}{(2\pi)^3} G_{22}(k) \quad (\text{B3b})$$

Prior to utilizing the effective potential  $V_{\text{eff}}$  for any computational purposes, it is imperative to engage in a brief discourse regarding its behavior under various loop approximation conditions. This discussion will provide

valuable insights into the applicability and limitations of  $V_{\text{eff}}$  within different theoretical frameworks.

### 1. Zero-loop

In zero-loop approximation, we solely consider the first diagram depicted in Fig. 2 as the contribution to  $\Phi[\phi_0]$ . Consequently, the effective potential can be succinctly expressed as  $V_{\text{eff}}[\phi_0] = -\frac{\mu}{2}\phi_0^2 + \frac{g_0}{8}\phi_0^4$ . Notably,  $V_{\text{eff}}[\phi_0]$  involves a single variable  $\phi_0$ , which represents the mean-field. By minimizing the  $V_{\text{eff}}[\phi_0]$  with respect to  $\phi_0$  and incorporating thermodynamic relationships, we derive  $\mu = g_0\rho$  and  $\rho = \frac{g_0}{2}\phi_0^2$ . These results align perfectly with the well-established findings within the mean-field approximation framework.

### 2. One-loop

Subsequently, we proceed to truncate  $\Phi[\phi_0, G]$  within one-loop approximation. This entails focusing solely on the diagrams featured in the first line of Fig. 2. Under this approximation, the effective potential  $V_{\text{eff}}[\phi_0, G]$  takes on a specific form, which can be written as

$$\begin{aligned} V_{\text{eff}}[\phi_0, G] = & -\frac{\mu}{2}\phi_0^2 + \frac{g_0}{8}\phi_0^4 \\ & + \frac{1}{2} \int_{\beta} \text{Tr} [\ln G^{-1}(k) + D_0^{-1}(k)G(k) - \mathbf{1}] \\ & + \frac{3g_0}{4}\phi_0^2 P_{11} + \frac{g_0}{4}\phi_0^2 P_{22} + \frac{g_2}{2}\phi_0^2 k^2 P_{11}. \end{aligned} \quad (\text{B4})$$

In Equation (B4),  $D_0^{-1}(k)$  can be written as

$$D_0^{-1}(k) = \begin{bmatrix} \frac{\hbar^2 k^2}{2m} - \mu & -\omega_n \\ \omega_n & \frac{\hbar^2 k^2}{2m} - \mu \end{bmatrix}, \quad (\text{B5})$$

being the inversion propagator in free space. And  $G(k)$  is the propagator of the system. Notably, Equation (B4) admits simplification by consolidating the terms in the third line into the second line. Through meticulous calculations, we can re-express  $V_{\text{eff}}[\phi_0, G]$  in a more concise form as

$$\begin{aligned} V_{\text{eff}}[\phi_0, G] = & -\frac{\mu}{2}\phi_0^2 + \frac{g_0}{8}\phi_0^4 \\ & + \frac{1}{2} \int_{\beta} \text{Tr} [\ln G^{-1}(k) + G_0^{-1}(k)G(k) - \mathbf{1}] \end{aligned} \quad (\text{B6})$$

where  $G_0^{-1}(k)$  is

$$G_0^{-1}(k) = \begin{bmatrix} \frac{\hbar^2 k^2}{2m} - \mu + \frac{3g_0}{2}\phi_0^2 + g_2\phi_0^2 k^2 & -\omega_n \\ \omega_n & \frac{\hbar^2 k^2}{2m} - \mu + \frac{g_0}{2}\phi_0^2 \end{bmatrix}, \quad (\text{B7})$$

being the inversion propagator within one-loop approximation. Minimizing the effective potential density  $V_{\text{eff}}[\phi_0, G]$  with respect to the elements of the propagator

$G(k)$ , we obtain that  $G^{-1}(k) = G_0^{-1}(k)$ . Consequently, we reformulate  $V_{\text{eff}}[\phi_0, G]$  as  $V_{\text{eff}}[\phi_0, G_0]$ , which in this approximation takes the form:  $V_{\text{eff}}[\phi_0, G_0] = -\frac{\mu}{2}\phi_0^2 + \frac{g_0}{8}\phi_0^4 + \frac{1}{2} \int_{\beta} \text{Tr} [\ln G_0^{-1}(k)]$ . Further minimization of  $V_{\text{eff}}[\phi_0, G_0]$  with respect to order parameter  $\phi_0$  and application of thermodynamic relationships lead to the quantum depletion:  $\rho_{\text{ex}} = \frac{8\rho}{3\sqrt{\pi}} (\rho a_s^3)^{1/2} - 64\sqrt{\pi}\rho \frac{r_s}{a_s} (\rho a_s^3)^{3/2}$ . This result aligns with the findings reported in Ref. [30], thereby validating the one-loop approximation approach.

### 3. Two-loop

Upon substituting the expression of  $\Phi[\phi_0, G]$  into the Eq. (B2), which encompasses all the diagrams depicted in Fig. 2, we are able to recast  $V_{\text{eff}}$  in an alternative form as

$$\begin{aligned} V_{\text{eff}}[\phi_0, G] = & -\frac{\mu}{2}\phi_0^2 + \frac{g_0}{8}\phi_0^4 \\ & + \frac{1}{2} \int_{\beta} \text{Tr} [\ln G^{-1}(k) + G_0^{-1}(k)G(k) - \mathbf{1}] \\ & + \frac{3g_0}{8}(P_{11}^2 + P_{22}^2) + \frac{g_0}{4}P_{11}P_{22}. \end{aligned} \quad (\text{B8})$$

In equation (B8),  $G(k)$  is the propagator or Green's function. By minimizing the CJT effective potential density  $V_{\text{eff}}[\phi_0, G]$  concerning the elements of the propagator  $G(k)$ , we obtain

$$G^{-1}(k) = G_0^{-1}(k) + \Sigma, \quad (\text{B9})$$

in which

$$\Sigma = \begin{bmatrix} \Sigma_1 & 0 \\ 0 & \Sigma_2 \end{bmatrix}, \quad (\text{B10})$$

with the matrix entries  $\Sigma_1$  and  $\Sigma_2$  being the self-energies that can be constructed from Eqs. (B8), (B3a), and (B3b),

$$\Sigma_1 = \frac{3g_0}{2}P_{11} + \frac{g_0}{2}P_{22}, \quad (\text{B11a})$$

$$\Sigma_2 = \frac{3g_0}{2}P_{22} + \frac{g_0}{2}P_{11}. \quad (\text{B11b})$$

Furthermore, the expression for  $G_0^{-1}(k)$  remains identical to that presented in Eq. (B7) in Appendix B2. Consequently, by examining the poles of the Green's function, as detailed in Ref. [59], we can derive the dispersion relation, which is given as

$$\begin{aligned} \epsilon_k = & \left( \frac{\hbar^2 k^2}{2m} - \mu + \frac{3g_0}{2}\phi_0^2 + g_2\phi_0^2 k^2 + \Sigma_1 \right)^{1/2} \\ & \times \left( \frac{\hbar^2 k^2}{2m} - \mu + \frac{g_0}{2}\phi_0^2 + \Sigma_2 \right)^{1/2}. \end{aligned} \quad (\text{B12})$$

By optimizing the CJT effective potential density with respect to the order parameter  $\phi_0$ , we can derive the gap

equation within the Hartree-Fock (HF) approximation,

$$-\mu + \frac{g_0}{2}\phi_0^2 + \Sigma_1 = 0. \quad (\text{B13})$$

The Goldstone theorem [60] postulates the necessity of a gapless excitation spectrum. Nevertheless, the dispersion relation derived from Eqs. (B12) and (B13) indicates a non-gapless spectrum, thereby violating the Goldstone theorem in the context of spontaneously broken symmetry within the HF approximation. To rectify this bug and reinstate the Nambu-Goldstone boson, we introduce a corrective term, denoted as  $\Delta V$  [58] to the  $V_{\text{eff}}[\phi_0, G]$ , which is given by

$$\Delta V = -\frac{g_0}{4}(P_{11}^2 + P_{22}^2) + \frac{g_0}{2}P_{11}P_{22}. \quad (\text{B14})$$

So that the revised  $V_{\text{eff}}$  is

$$\begin{aligned} V_{\text{eff}} = & -\frac{\mu}{2}\phi_0^2 + \frac{g_0}{8}\phi_0^4 \\ & + \frac{1}{2}\int_{\beta}\text{Tr}[\ln G^{-1}(k) + G_0^{-1}(k)G(k) - \mathbf{1}] \\ & + \frac{g_0}{8}(P_{11}^2 + P_{22}^2) + \frac{3g_0}{4}P_{11}P_{22}. \end{aligned} \quad (\text{B15})$$

In Equation (B15), the first two terms constitute the mean-field component, corresponding to the condensate atoms, while the subsequent terms represent the excitation part stemming from the excited atoms. By replicating the calculations performed leading up to Eq. (B9), we obtain the revised inverse propagator,

$$G^{-1}(k) = G_0^{-1}(k) + \Sigma', \quad (\text{B16})$$

where

$$\Sigma' = \begin{bmatrix} \Sigma'_1 & 0 \\ 0 & \Sigma'_2 \end{bmatrix}, \quad (\text{B17})$$

in which the self-energies  $\Sigma'_1$  and  $\Sigma'_2$  are defined as follows,

$$\Sigma'_1 = \frac{g_0}{2}P_{11} + \frac{3g_0}{2}P_{22}, \quad (\text{B18a})$$

$$\Sigma'_2 = \frac{g_0}{2}P_{22} + \frac{3g_0}{2}P_{11}. \quad (\text{B18b})$$

Then, the gap equation that  $\mu$  satisfies can be reformulated as

$$-\mu + \frac{g_0}{2}\phi_0^2 + \Sigma'_2 = 0. \quad (\text{B19})$$

Furthermore, we can formulate the Schwinger-Dyson (SD) equation as

$$-\mu + \frac{3g_0}{2}\phi_0^2 + \Sigma'_1 = M^2. \quad (\text{B20})$$

Upon modifying  $m$  to  $m^* = m/(1 + 2mg_2\phi_0^2/\hbar^2)$ , the revised inversion propagator  $G^{-1}(k)$  and the corresponding propagator  $G(k)$  can be turned out

$$G^{-1}(k) = \begin{bmatrix} \frac{\hbar^2 k^2}{2m^*} + M^2, & -\omega_n \\ \omega_n, & \frac{k^2}{2m} \end{bmatrix}, \quad (\text{B21a})$$

$$G(k) = \frac{1}{\epsilon_k^2 + \omega_n^2} \begin{bmatrix} \frac{\hbar^2 k^2}{2m}, & \omega_n \\ -\omega_n, & \frac{\hbar^2 k^2}{2m^*} + M^2 \end{bmatrix}. \quad (\text{B21b})$$

In Equation (B21b),  $\epsilon_k = \sqrt{\frac{\hbar^2 k^2}{2m}(\frac{\hbar^2 k^2}{2m^*} + M^2)}$ , representing the dispersion relation.

Plugging Eqs. (B7) and (B21b) into Eq. (B15) and performing the calculations pertaining to the second term, we proceed to obtain

$$\begin{aligned} V_{\text{eff}} = & -\frac{\mu}{2}\phi_0^2 + \frac{g_0}{8}\phi_0^4 \\ & + \frac{1}{2}\int_{\beta}\text{Tr}[\ln G^{-1}(k)] \\ & + \frac{g_0}{8}(P_{11}^2 + P_{22}^2) + \frac{3g_0}{4}P_{11}P_{22} \\ & + \frac{1}{2}\left(-\mu + \frac{3g_0}{2}\phi_0^2 - M^2\right)P_{11} \\ & + \frac{1}{2}\left(-\mu + \frac{g_0}{2}\phi_0^2\right)P_{22}. \end{aligned} \quad (\text{B22})$$

Meanwhile, by evaluating Eq. (B3) through summing over the bosonic Matsubara frequencies using Eq. (B21b), and then taking the limit as  $T \rightarrow 0$ , we perform the calculations in spherical coordinates employing dimensional

regularization techniques, yielding:

$$\begin{aligned}
P_{11} &= \frac{1}{2} \int \frac{d\mathbf{k}}{(2\pi)^3} \sqrt{\frac{\frac{\hbar^2 k^2}{2m}}{\frac{\hbar^2 k^2}{2m^*} + M^2}} \\
&= \frac{1}{2} \int \frac{d\mathbf{k}}{(2\pi)^3} \sqrt{\frac{\frac{\hbar^2 k^2}{2m}}{\frac{\hbar^2 k^2}{2m^*} + M^2}} \sqrt{\frac{m^*}{m}} \\
&= \frac{1}{8\pi^2} \left( \frac{2m^* M^2}{\hbar^2} \right)^{\frac{3}{2}} \sqrt{\frac{m^*}{m}} \int_0^\infty t(t+1)^{-\frac{1}{2}} dt \\
&= \frac{1}{8\pi^2} \left( \frac{2m^* M^2}{\hbar^2} \right)^{\frac{3}{2}} \sqrt{\frac{m^*}{m}} \frac{\Gamma[2] \Gamma[\frac{-3}{2}]}{\Gamma[\frac{1}{2}]} \\
&= \frac{\sqrt{2} m^{*3/2} M^3}{3\pi^2 \hbar^3} \sqrt{\frac{m^*}{m}}, \tag{B23a}
\end{aligned}$$

$$\begin{aligned}
P_{22} &= \frac{1}{2} \int \frac{d\mathbf{k}}{(2\pi)^3} \sqrt{\frac{\frac{\hbar^2 k^2}{2m}}{\frac{\hbar^2 k^2}{2m^*} + M^2}} \\
&= \frac{1}{2} \int \frac{d\mathbf{k}}{(2\pi)^3} \sqrt{\frac{\frac{\hbar^2 k^2}{2m}}{\frac{\hbar^2 k^2}{2m^*} + M^2}} \sqrt{\frac{m}{m^*}} \\
&= \frac{1}{8\pi^2} \left( \frac{2m^* M^2}{\hbar^2} \right)^{\frac{3}{2}} \sqrt{\frac{m}{m^*}} \int_0^\infty t^0 (t+1)^{\frac{1}{2}} dt \\
&= \frac{1}{8\pi^2} \left( \frac{2m^* M^2}{\hbar^2} \right)^{\frac{3}{2}} \sqrt{\frac{m}{m^*}} \frac{\Gamma[1] \Gamma[\frac{-3}{2}]}{\Gamma[-\frac{1}{2}]} \\
&= -\frac{m^{*3/2} M^3}{3\sqrt{2}\pi^2 \hbar^3} \sqrt{\frac{m}{m^*}}. \tag{B23b}
\end{aligned}$$

### Appendix C: DETAILED CALCULATION OF THE SOLUTION OF EQ. (13)

For the sake of self-consistence of this work, we briefly review the key steps to solve the Eq. (13) utilizing perturbation theory. Initially, we introduce a small parameter  $\epsilon$  to the left-hand side of  $M^3$ , thereby transforming the cubic equation in  $M$  into the form

$$\begin{aligned}
\epsilon M^3 + \frac{3\pi\hbar(1+4\frac{mg_2}{\hbar^2}\rho)^{3/2}}{8\sqrt{2}a_s m^{*1/2}} M^2 \\
- \frac{3\pi^2 \hbar^3 (1+4\frac{mg_2}{\hbar^2}\rho)^{1/2}}{\sqrt{2}m^{*3/2}} \rho = 0. \tag{C1}
\end{aligned}$$

$$M = \sqrt{2g_0\rho} \left\{ 1 - \frac{16}{3\sqrt{\pi} (1+4\frac{mg_2}{\hbar^2}\rho)^2} \sqrt{\rho a_s^3} \left[ 1 - \frac{40}{3\sqrt{\pi} (1+4\frac{mg_2}{\hbar^2}\rho)^2} \sqrt{\rho a_s^3} \right] + \mathcal{O}[(\rho a_s^3)^{3/2}] \right\}. \tag{C9}$$

Meanwhile, we express  $M$  as a polynomial expansion in terms of the parameter  $\epsilon$

$$M \rightarrow M_0 + \epsilon M_1 + \epsilon^2 M_2. \tag{C2}$$

Next, we substitute the expression for  $M$  from Eq. (C2) into Eq. (C1) and organize the resulting equation into orders of  $\epsilon^0$ ,  $\epsilon^1$  and  $\epsilon^2$ .

(i)  $\epsilon^0$  order of equation

$$\frac{3\pi\hbar(1+4\frac{mg_2}{\hbar^2}\rho)^{3/2}}{8\sqrt{2}a_s m^{*1/2}} M_0^2 - \frac{3\pi^2 \hbar^3 (1+4\frac{mg_2}{\hbar^2}\rho)^{1/2}}{\sqrt{2}m^{*3/2}} \rho = 0, \tag{C3}$$

$$\Rightarrow M_0 = \sqrt{2g_0\rho}. \tag{C4}$$

(ii)  $\epsilon^1$  order of equation

$$M_0^3 + \frac{3\pi\hbar(1+4\frac{mg_2}{\hbar^2}\rho)^{3/2}}{4\sqrt{2}a_s m^{*1/2}} M_0 M_1 = 0, \tag{C5}$$

$$\Rightarrow M_1 = -\frac{16\sqrt{2g_0\rho}}{3\sqrt{\pi} (1+4\frac{mg_2}{\hbar^2}\rho)^2} \sqrt{\rho a_s^3}. \tag{C6}$$

(iii)  $\epsilon^2$  order of equation

$$3M_0^2 M_1 + \frac{3\pi\hbar(1+4\frac{mg_2}{\hbar^2}\rho)^{3/2}}{8\sqrt{2}a_s m^{*1/2}} (M_1^2 + 2M_0 M_2) = 0, \tag{C7}$$

$$\Rightarrow M_2 = \frac{640\sqrt{2g_0\rho}}{9\pi (1+4\frac{mg_2}{\hbar^2}\rho)^4} \rho a_s^3. \tag{C8}$$

Finally, we derive the expression for  $M$ , which is expanded as  $M_0 + M_1 + M_2$ , in terms of the gas parameter  $\rho a_s^3$

[1] N. Nagaosa, *Quantum Field Theory in Condensed Matter Physics* (Springer Science & Business Media, 1999).

[2] L. Pitaevskii and S. Stringari, *Bose-Einstein Condensation and Superfluidity* (Oxford University Press, 2016).

- [3] M. E. Peskin, *An Introduction to Quantum Field Theory* (CRC Press, 1995).
- [4] A. Bulgac, Dilute quantum droplets, *Phys. Rev. Lett.* **89**, 050402 (2002).
- [5] D. S. Petrov, Quantum mechanical stabilization of a collapsing Bose-Bose mixture, *Phys. Rev. Lett.* **115**, 155302 (2015).
- [6] L. Tanzi, E. Lucioni, F. Famà, J. Catani, A. Fioretti, C. Gabbanini, R. N. Bisset, L. Santos, and G. Modugno, Observation of a dipolar quantum gas with metastable supersolid properties, *Phys. Rev. Lett.* **122**, 130405 (2019).
- [7] I. Ferrier-Barbut, H. Kadau, M. Schmitt, M. Wenzel, and T. Pfau, Observation of quantum droplets in a strongly dipolar Bose gas, *Phys. Rev. Lett.* **116**, 215301 (2016).
- [8] L. Chomaz, S. Baier, D. Petter, M. J. Mark, F. Wächtler, L. Santos, and F. Ferlaino, Quantum-fluctuation-driven crossover from a dilute Bose-Einstein condensate to a macrodroplet in a dipolar quantum fluid, *Phys. Rev. X* **6**, 041039 (2016).
- [9] M. Wenzel, F. Böttcher, T. Langen, I. Ferrier-Barbut, and T. Pfau, Striped states in a many-body system of tilted dipoles, *Phys. Rev. A* **96**, 053630 (2017).
- [10] G. Semeghini, G. Ferioli, L. Masi, C. Mazzinghi, L. Wolswijk, F. Minardi, M. Modugno, G. Modugno, M. Inguscio, and M. Fattori, Self-bound quantum droplets of atomic mixtures in free space, *Phys. Rev. Lett.* **120**, 235301 (2018).
- [11] C. R. Cabrera, L. Tanzi, J. Sanz, B. Naylor, P. Thomas, P. Cheiney, and L. Tarruell, Quantum liquid droplets in a mixture of Bose-Einstein condensates, *Science* **359**, 301 (2018).
- [12] C. D'Errico, A. Burchianti, M. Prevedelli, L. Salasnich, F. Ancilotto, M. Modugno, F. Minardi, and C. Fort, Observation of quantum droplets in a heteronuclear bosonic mixture, *Phys. Rev. Res.* **1**, 033155 (2019).
- [13] T. D. Lee, K. Huang, and C. N. Yang, Eigenvalues and eigenfunctions of a Bose system of hard spheres and its low-temperature properties, *Phys. Rev.* **106**, 1135 (1957).
- [14] T. D. Lee and C. N. Yang, Many-body problem in quantum mechanics and quantum statistical mechanics, *Phys. Rev.* **105**, 1119 (1957).
- [15] F. Dalfovo, S. Giorgini, L. P. Pitaevskii, and S. Stringari, Theory of Bose-Einstein condensation in trapped gases, *Rev. Mod. Phys.* **71**, 463 (1999).
- [16] R. Roth and H. Feldmeier, Effective s- and p-wave contact interactions in trapped degenerate Fermi gases, *Phys. Rev. A* **64**, 043603 (2001).
- [17] T. T. Wu, Ground state of a Bose system of hard spheres, *Phys. Rev.* **115**, 1390 (1959).
- [18] N. Van Thu and J. Berx, The condensed fraction of a homogeneous dilute Bose gas within the improved Hartree-Fock approximation, *J. Stat. Phys.* **188**, 16 (2022).
- [19] C. Mordini, D. Trypogeorgos, A. Farolfi, L. Wolswijk, S. Stringari, G. Lamporesi, and G. Ferrari, Measurement of the canonical equation of state of a weakly interacting 3D Bose gas, *Phys. Rev. Lett.* **125**, 150404 (2020).
- [20] T. G. Skov, M. G. Skou, N. B. Jørgensen, and J. J. Arlt, Observation of a Lee-Huang-Yang fluid, *Phys. Rev. Lett.* **126**, 230404 (2021).
- [21] L. Lavoine, A. Hammond, A. Recati, D. S. Petrov, and T. Bourdel, Beyond-mean-field effects in Rabi-coupled two-component Bose-Einstein condensate, *Phys. Rev. Lett.* **127**, 203402 (2021).
- [22] R. Cominotti, A. Berti, C. Dulin, C. Rogora, G. Lamporesi, I. Carusotto, A. Recati, A. Zenesini, and G. Ferrari, Ferromagnetism in an extended coherently coupled atomic superfluid, *Phys. Rev. X* **13**, 021037 (2023).
- [23] E. Busley, L. E. Miranda, A. Redmann, C. Kurtscheid, K. K. Umesh, F. Vewinger, M. Weitz, and J. Schmitt, Compressibility and the equation of state of an optical quantum gas in a box, *Science* **375**, 1403 (2022), <https://www.science.org/doi/pdf/10.1126/science.abm2543>.
- [24] I. Bloch, J. Dalibard, and W. Zwerger, Many-body physics with ultracold gases, *Rev. Mod. Phys.* **80**, 885 (2008).
- [25] E. Braaten, H.-W. Hammer, and S. Hermans, Nonuniversal effects in the homogeneous Bose gas, *Phys. Rev. A* **63**, 063609 (2001).
- [26] A. Cappellaro and L. Salasnich, Thermal field theory of bosonic gases with finite-range effective interaction, *Phys. Rev. A* **95**, 033627 (2017).
- [27] F. Lorenzi, A. Bardin, and L. Salasnich, On-shell approximation for the s-wave scattering theory, *Phys. Rev. A* **107**, 033325 (2023).
- [28] X. Ye, T. Yu, and Z. Liang, Nonuniversal equation of state of a quasi-two-dimensional Bose gas in dimensional crossover, *Phys. Rev. A* **109**, 063304 (2024).
- [29] T. Yu, X. Ye, and Z. Liang, Interaction-induced dimensional crossover from fully three-dimensional to one-dimensional spaces, *Phys. Rev. A* **110**, 013304 (2024).
- [30] A. Tononi, A. Cappellaro, and L. Salasnich, Condensation and superfluidity of dilute Bose gases with finite-range interaction, *New J. Phys.* **20**, 125007 (2018).
- [31] S. L. Cornish, N. R. Claussen, J. L. Roberts, E. A. Cornell, and C. E. Wieman, Stable  $^{85}\text{Rb}$  Bose-Einstein condensates with widely tunable interactions, *Phys. Rev. Lett.* **85**, 1795 (2000).
- [32] S. Cowell, H. Heiselberg, I. E. Mazets, J. Morales, V. R. Pandharipande, and C. J. Pethick, Cold Bose gases with large scattering lengths, *Phys. Rev. Lett.* **88**, 210403 (2002).
- [33] C. Chin, R. Grimm, P. Julienne, and E. Tiesinga, Feshbach resonances in ultracold gases, *Rev. Mod. Phys.* **82**, 1225 (2010).
- [34] H. Wu and J. E. Thomas, Optical control of Feshbach resonances in Fermi gases using molecular dark states, *Phys. Rev. Lett.* **108**, 010401 (2012).
- [35] H. Wu and J. E. Thomas, Optical control of the scattering length and effective range for magnetically tunable Feshbach resonances in ultracold gases, *Phys. Rev. A* **86**, 063625 (2012).
- [36] O. Morsch and M. Oberthaler, Dynamics of Bose-Einstein condensates in optical lattices, *Rev. Mod. Phys.* **78**, 179 (2006).
- [37] S. Stringari, Collective excitations of a trapped Bose-condensed gas, *Phys. Rev. Lett.* **77**, 2360 (1996).
- [38] L. Pitaevskii and S. Stringari, Elementary excitations in trapped Bose-Einstein condensed gases beyond the mean-field approximation, *Phys. Rev. Lett.* **81**, 4541 (1998).
- [39] J. M. Cornwall, R. Jackiw, and E. Tomboulis, Effective action for composite operators, *Phys. Rev. D* **10**, 2428 (1974).
- [40] G. Amelino-Camelia and S.-Y. Pi, Self-consistent improvement of the finite-temperature effective potential, *Phys. Rev. D* **47**, 2356 (1993).
- [41] A. Pilaftsis and D. Teresi, Symmetry-improved CJT ef-

- fective action, *Nucl. Phys. B* **874**, 594 (2013).
- [42] A. Sharma, G. Kartvelishvili, and J. Khoury, Finite temperature description of an interacting Bose gas, *Phys. Rev. D* **106**, 045025 (2022).
- [43] L. Salasnich, Nonuniversal equation of state of the two-dimensional Bose gas, *Phys. Rev. Lett.* **118**, 130402 (2017).
- [44] L. Salasnich and F. Toigo, Zero-point energy of ultracold atoms, *Phys. Rep.* **640**, 1 (2016).
- [45] T. Haugset, H. Haugerud, and F. Ravndal, Thermodynamics of a weakly interacting Bose-Einstein gas, *Ann. Phys.* **266**, 27 (1998).
- [46] T. H. Phat, L. V. Hoa, N. T. Anh, and N. Van Long, Bose-Einstein condensation in binary mixture of Bose gases, *Ann. Phys.* **324**, 2074 (2009).
- [47] T. H. Phat, L. V. Hoa, N. T. Anh, and N. V. Long, High temperature symmetry nonrestoration and inverse symmetry breaking in the Cornwall-Jackiw-Tomboulis formalism, *Phys. Rev. D* **76**, 125027 (2007).
- [48] T. H. Phat, N. Van Long, N. T. Anh, and L. V. Hoa, Kaon condensation in the linear sigma model at finite density and temperature, *Phys. Rev. D* **78**, 105016 (2008).
- [49] P. T. Song, Universal quantum effect of two-body correlation in a weakly interacting Bose gas, *Europhys. Lett.* **139**, 45001 (2022).
- [50] T. Bourdel, L. Khaykovich, J. Cubizolles, J. Zhang, F. Chevy, M. Teichmann, L. Tarruell, S. J. J. M. F. Kokkelmans, and C. Salomon, Experimental study of the BEC-BCS crossover region in Lithium 6, *Phys. Rev. Lett.* **93**, 050401 (2004).
- [51] G. E. Astrakharchik, R. Combescot, X. Leyronas, and S. Stringari, Equation of state and collective frequencies of a trapped Fermi gas along the BEC-unity crossover, *Phys. Rev. Lett.* **95**, 030404 (2005).
- [52] Y. Hu, Z. Liang, and B. Hu, Collective excitations of a trapped Bose-Einstein condensate in the presence of weak disorder and a two-dimensional optical lattice, *Phys. Rev. A* **81**, 053621 (2010).
- [53] Y. Hu and Z. Liang, Visualization of dimensional effects in collective excitations of optically trapped quasi-two-dimensional Bose gases, *Phys. Rev. Lett.* **107**, 110401 (2011).
- [54] Y. Li and S. Stringari, Universal contact and collective excitations of a strongly interacting Fermi gas, *Phys. Rev. A* **84**, 023628 (2011).
- [55] Y. Hu, Z. Liang, and B. Hu, Effects of disorder on quantum fluctuations and superfluid density of a Bose-Einstein condensate in a two-dimensional optical lattice, *Phys. Rev. A* **80**, 043629 (2009).
- [56] M. Bartenstein, A. Altmeyer, S. Riedl, R. Geursen, S. Jochim, C. Chin, J. H. Denschlag, R. Grimm, A. Simoni, E. Tiesinga, C. J. Williams, and P. S. Julienne, Precise determination of  $^6\text{Li}$  cold collision parameters by radio-frequency spectroscopy on weakly bound molecules, *Phys. Rev. Lett.* **94**, 103201 (2005).
- [57] H. Wu and J. E. Thomas, Optical control of the scattering length and effective range for magnetically tunable Feshbach resonances in ultracold gases, *Phys. Rev. A* **86**, 063625 (2012).
- [58] Y. B. Ivanov, F. Riek, and J. Knoll, Gapless Hartree-Fock resummation scheme for the  $O(N)$  model, *Phys. Rev. D* **71**, 105016 (2005).
- [59] J. O. Andersen, Theory of the weakly interacting Bose gas, *Rev. Mod. Phys.* **76**, 599 (2004).
- [60] J. Goldstone, A. Salam, and S. Weinberg, Broken symmetries, *Phys. Rev.* **127**, 965 (1962).